ORGANIC CHEMISTRY

FRONTIERS

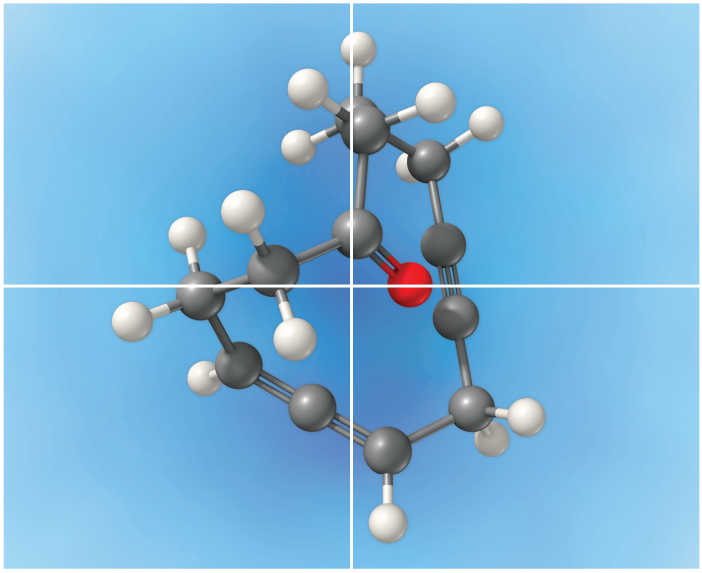

Accepted Manuscript

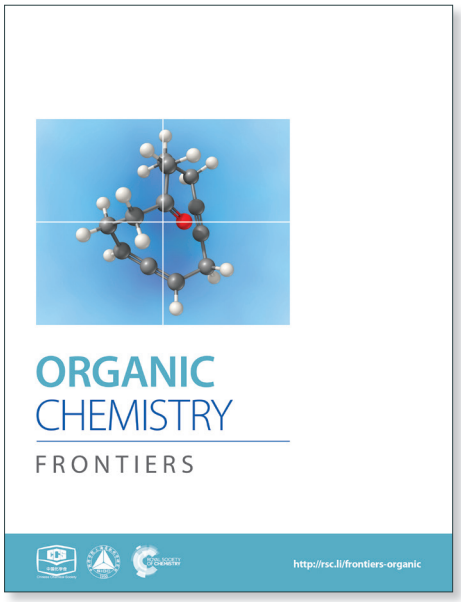

This is an *Accepted Manuscript*, which has been through the Royal Society of Chemistry peer review process and has been accepted for publication.

Accepted Manuscripts are published online shortly after acceptance, before technical editing, formatting and proof reading. Using this free service, authors can make their results available to the community, in citable form, before we publish the edited article. We will replace this *Accepted Manuscript* with the edited and formatted *Advance Article* as soon as it is available.

You can find more information about *Accepted Manuscripts* in the **Information for Authors**.

Please note that technical editing may introduce minor changes to the text and/or graphics, which may alter content. The journal's standard **Terms & Conditions** and the **Ethical guidelines** still apply. In no event shall the Royal Society of Chemistry be held responsible for any errors or omissions in this *Accepted Manuscript* or any consequences arising from the use of any information it contains.

Organic Chemistry Frontiers

RSCPublishing

ARTICLE

Synthesis and Photophysics of a Broadband Absorbing Texaphyrin Derivative Bearing Rhodamine 6G Motif

Lei Hu,[a,b] Chengkui Pei,[a] Zhongjing Li,[a] Chengzhe Wang,[a] Guichun Yang[b] and Wenfang Sun[a,*]

Cite this: DOI: 10.1039/xoxxoooooox

Received ooth January 2014,
Accepted ooth xxxx 2014

DOI: 10.1039/xoxxoooooox

www.rsc.org/

A texaphyrin derivative with Rhodamine 6G attached (complex **11**) via a C≡C bond was synthesized and characterized. The UV-vis absorption, emission and nanosecond transient absorption (TA) characteristics of this complex were systematically studied in acetone solutions. The photophysics of this complex was also compared to those of its precursor compounds texaphyrin **12** and **13** and Rhodamine 6G derivative **3**. The UV-vis absorption spectrum of **11** consists of both the characteristic Soret and Q-like bands of texaphyrin derivative **13** and the identical absorption band from Rhodamine 6G derivative **3**. When excited at 550 nm (the major absorption band of Rhodamine 6G), **11** exhibits fluorescence bands from both Rhodamine 6G component (582 nm) and texaphyrin component (802 nm), but the intensity of the 582 nm band is dramatically reduced accompanied by a significant increase of the 802 nm band compared to those from **3** and **13**, indicating electron / energy transfer from the singlet excited state of Rhodamine 6G. The ns TA spectrum of **11** resembles that of texaphyrin derivative **13** but with both the bleaching band and absorption band red-shifted. The triplet lifetimes deduced from the decay of ns TA are quite similar for **11**, **12** and **13**, indicating the lack of interactions between the triplet excited states of texaphyrin component and the Rhodamine 6G component. The broadband ground-state absorption of **11** from the visible to the near-IR region, and the possible electron / energy transfer from the singlet excited state of Rhodamine 6G component to the texaphyrin component suggest that this complex could potentially be a broadband photosensitizer for dye-sensitized solar cell applications.

Introduction

Dye-sensitized solar cells (DSSCs) are considered as the most promising innovative solar energy conversion technology due to high incident solar light-to-electricity conversion efficiency (η) and low cost of production.[1] To date, ruthenium polypyridyl-based complexes are still one of the most efficient sensitizers with the highest η value of 11.5%.[2] However, the ruthenium sensitizers are toxic, expensive and display relatively low molar absorptivity especially in the near-IR region.[3,4] To expand the absorption spectral region of DSSCs, great efforts have been put to the development of cyclic tetrapyrrole-based molecules,[5,6] including porphyrins,[7] chlorins,[8] bacteriochlorins,[9] and phthalocyanines.[10] The interest in tetrapyrrole-based molecules is based on their extremely intense Soret band in the visible spectral region and their readily tunable Q bands. It is possible to red-shift the Q bands to the near-IR region by expanding the π-conjugation of the macrocyclic ligand,[11] introducing different functional groups on the pyrrole moiety, axial ligation of the central metal,[12] and coordination with different central metals (Mg, Zn, Fe, Ni, Cu, Pd, etc.).[13] Although the Q-band could be red-shifted, the highest η value of the cell based on bacteriochlorins sensitizers was no more than 7.1%.[9] It was reported that the increased probability of exciton annihilation from porphyrins in proximity could be accounted for the lower efficiency because porphyrins have an inherent tendency to aggregate.[14] However, in recent years, Grätzel and co-workers reported that the efficiency of mesoscopic dye-sensitized solar cells based on donor–acceptor-substituted porphyrins could reach 11-12%,[15,16] which exceeds the efficiency of Ru complex based DSSCs.

Texaphyrins are pentaazadentate porphyrin-like aromatic macrocycles with extended π-conjugations and approximately 20% larger core size than porphyrins.[17-19] They can coordinate with large metal ions to form almost coplanar configurations. As a result, the Q-band of texaphyrins could be bathochromically shifted to above 800 nm with appropriate diaminoarene precursor,[20,21] which makes it possible to efficiently absorb the solar energy in both the high energy and near-IR regions. However, due to the red-shifted Q-band, there appears to be a larger window (~ 500 – 700 nm) between the Soret and the Q bands, which makes it insufficient to harvest light in the visible spectral region between 500 and 680 nm.[22] For an ideal DSSC sensitizer, it is required that the absorption of the sensitizer

should cover the full visible to near-IR spectral region. To improve the light-harvesting efficiency in the visible spectral region, we propose to introduce Rhodamine 6G that absorbs light intensely between 500 and 600 nm[23,24] to the texaphyrin macrocycle by a C≡C linker to facilitate the conjugation between the texaphyrin macrocycle and Rhodamine 6G and allow for the possible electron or energy transfer from the Rhodamine 6G to texaphyrin or vice versa to occur. It is expected that the absorption from the attached Rhodamine 6G could fill in the gap between the Soret and Q bands in texaphyrins and thus sufficiently increase the light-harvesting ability of texaphyrins in the visible region.

The structure of the target texaphyrin derivative (complex **11**) with attached Rhodamine 6G is shown in Chart 1 and the synthetic route for this complex is outlined in Scheme 1. The UV-vis absorption, emission and triplet transient absorption characteristics of complex **11** are investigated and reported in this paper. For comparison purpose, the photophysics of the parent texaphyrin complexes (**12** and **13**) and ethynyl Rhodamine 6G (compound **3**) were also studied and reported herewith. A point worthy of mentioning is that this paper only focuses on the synthesis and photophysics of the new texaphyrin derivative **11**, its application in DSSC will be studied and reported later.

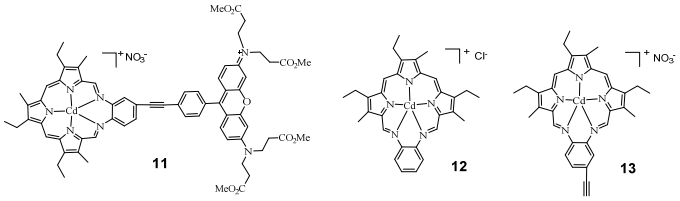

Chart 1. Structures for the target complex **11** and the parent texaphyrins **12** and **13**.

Results and discussion

Synthesis. The general procedure for the synthesis of Rhodamine 6G pendant texaphyrin derivative **11** follows the procedure originally reported by Sessler *et. al.* for texaphyrins,[17] namely using the acid-catalyzed Schiff base condensation reaction between the Rhodamine 6G ethynyl substituted benzene diamine (**5b**) and diformyltripyrrane (**9**) to form the macrocyclic ligand (**10**). Then **10** reacts with cadmium salt at room temperature in air to form **11**. In this step, oxidation of the ligand and coordination with Cd^{2+} ion occur simultaneously. As shown in Scheme 1, the key precursor for the synthesis of **11** is the diamine precursor **5b**. Initially, we attempted to use Sonogashira coupling reaction between brominated Rhodamine 6G (**1**) and 4-ethynyl-2-nitroaniline (**2a**) or 4-ethynylbenzene-1,2-diamine (**2b**); or use ethynyl Rhodamine 6G (**3**) to react with 4-iodo-2-nitroaniline (**4a**) or 4-iodobenzene-1,2-diamine (**4b**). Unfortunately, none of the aforementioned combination yielded the desired product **5** regardless whether we used the standard Sonogashira coupling reaction conditions or modified conditions. Therefore, we adopted a new strategy to form the aldehyde precursor **7** with 4-ethynyl-2-nitroaniline attached first then convert it to the Rhodamine 6G derivative **5a**. Reduction of nitro substituent resulted in the desired precursor **5b**.

Compounds **1**,[25] **2a**,[26,27] **4a**,[28] **6**,[22,29] **8**,[30] and **9**[12] were synthesized according to the procedures reported in the literatures with some modifications. Sonogashira coupling reaction between 4-ethynylbenzaldehyde **6** and **4a** afforded compound **7** as an orange powder. Reaction of compounds **7** and **8** using *p*-TsOH as the catalyst, followed by oxidation using chloranil at room temperature for 2 hours gave compound **5a** in a very low yield (3.4%). **5a** was then reduced by Zn powder in the presence of NH_4Cl to afford the key precursor **5b**. During the synthesis of the macrocyclic ligand **10**, a water segregator was used to remove the water generated from the acid-catalyzed Schiff base condensation reaction between **5b** and diformyltripyrrane **9** in order to move the reaction equilibrium forward towards the product.[15] Because **10** was very difficult to be purified even after several times column purification and recrystallization, the crude product confirmed by HRMS was directly used for the next step reaction without further purification. Complex **11** was synthesized from **10** following the procedure reported for texaphyrins.[17,31] The reaction was monitored by UV-vis spectroscopy. During the reaction, the 375 nm peak corresponding to the ligand **10** gradually disappeared, while the Q band at ~770 nm originating from the conjugated metal complex kept increasing. The reaction was stopped when no more change of the Q band intensity was observed. The crude product was purified by silica gel column chromatography with 3.3-20% methanol in dichloromethane (v/v) as the eluent, and then recrystallized from methanol and ethyl acetate. The structure and purity of **11** were verified by ^1H and ^{13}C NMR, HRMS and elemental analysis.

The synthesis and characterization of the reference complex **12** has been reported previously.[32] The other reference complex **13** was obtained by acid-catalyzed Schiff base condensation reaction between the 4-ethynyl-1,2-diaminobenzene (**2b**) and diformyltripyrrane (**9**) to form the macrocyclic ligand first; then complexation with cadmium salt at room temperature in air yielded the complex **13**.

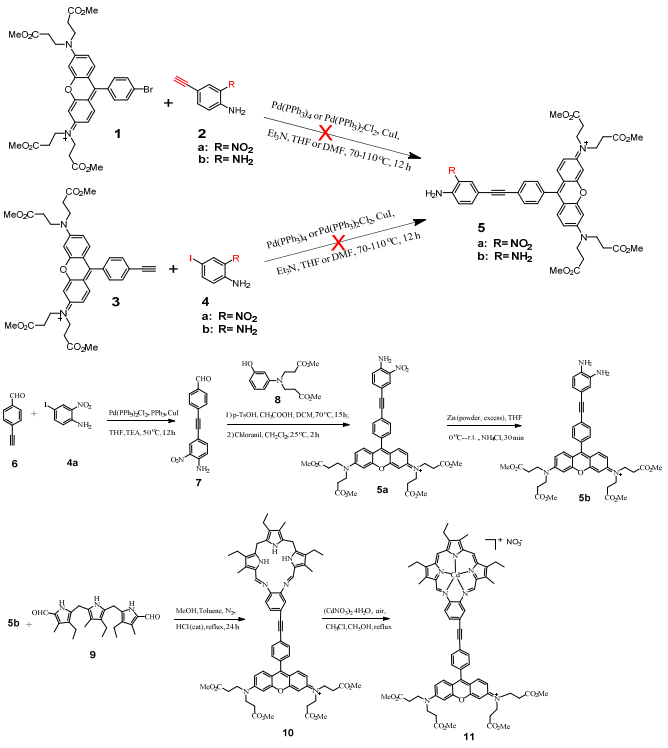

Scheme 1. Synthetic route for Rhodamine 6G pendant texaphyrin complex (**11**).

Electronic absorption. The UV-vis absorption spectra of **3, 11**, **12** and **13** in acetone are displayed in Figure 1a. Complex **11** exhibits three characteristic absorption bands: the Soret bands appear in the 400-500 nm region (λ_{max} = 464 nm, ε = 64,390 L.mol^{-1}.cm^{-1}), while the Q bands are in the near-IR region (λ_{max} = 772 nm, ε = 24,920 L.mol^{-1}.cm^{-1}). Compared to those of complex **12**, the Soret and Q bands of **11** exhibit a 45 and 15 nm bathochromic shift, respectively, and the molar extinction coefficients are also significant enhanced. This should be attributed to the increased π-conjugation in texaphyrin through triplet bond connection with Rhodamine 6G, which is confirmed by the similar energies and molar extinction coefficients as those of **13**. The most intense absorption band at 553 nm (ε = 89,780 L.mol^{-1}.cm^{-1}) appears at the identical position of the absorption band of **3**, thus is assigned to the $^1\pi,\pi^*$ transition from the Rhodamine 6G component. To understand whether the UV-vis absorption spectrum of **11** is a simple addition of the absorption from **3** and **12** or any interactions occur between these two components, we measured the absorption spectra of the mixture of equivalent **3** and **12** in acetone at the identical concentration of 1×10^{-5} mol/L, and the spectrum is compiled in Figure 1a as well. Comparing this spectrum to that of **11**, we find that the Soret and Q bands in **11** are pronouncedly red-shifted and the molar extinction coefficients are higher in comparison to those of the mixed solution of **3** and **12**; however, the absorption band at 553 nm remains the same position but with a slightly decreased molar extinction coefficient. The red-shift and increased molar extinction coefficient of **11** is again due to the extended π-conjugation by the triple bond. This is confirmed by the similar energies and molar extinction coefficients of the absorption bands in **11** to those in the mixed equivalent **3** and **13** in acetone at the identical concentration of 1×10^{-5} mol/L (see inset in Figure 1a). However, the new band at 464 nm in **11** should be due to the interactions between the Rhodamine 6G component and the texaphyrin component.

The concentration-dependency study shows that the UV-vis absorption of **11** obeys Lambert-Beer's law in the concentration range used in our study (1×10^{-6} to 1×10^{-4} mol/L), indicating that no ground-state aggregation occurs in this concentration range. The solvents-dependency UV-vis absorption spectra of **11** were also measured and the results are shown in Figure 1b. It appears that the absorption bands are slightly red-shifted in less polar solvent toluene. In CH_2Cl_2 solution, only the Q band shows somewhat red-shift in comparison to that in methanol. Although the minor solvatochromic effect of **11** is in accordance with the π,π^* transition nature of these bands, the observed negative solvatochromic effect implies that the excited state of **11** is slightly less polar than its ground state.

Photoluminescence. Figure 2a shows the fluorescence spectra of **3**, **11**, **12**, **13** and the mixture of equivalent **3** and **12** at the concentration of 1×10^{-5} mol/L in acetone when excited at the Q(0,0) band (*i.e.* 771 nm). For Rhodamine 6G derivative **3**, a strong emission appears at 582 nm, which is attributed to the two-photon induced upconverted fluorescence from **3**.[33] For the reference complexes **12** and **13**, the emission occurs at ca. 787 nm and 802 nm, respectively, which originates from the respective $^1\pi,\pi^*$ states of **12** and **13.** The equal-equivalent mixture of **3** and **12** at the same concentration of 1×10^{-5} mol/L gives an identical emission band at 787 nm to that of **12** and a slightly reduced-intensity band at 582 nm. The slightly weaker emission at 582 nm for the mixed **3** and **12** solution compared to that of **12** should be attributed to the reduced efficient excitation energy towards the upconversion fluorescence because both the texaphyrin and Rhodamine 6G are excited with the 771 nm light. Taking this factor into account, we can conclude that no interactions occur between **3** and **12** when they are physically mixed with each other. In contrast, when texaphyrin and Rhodamine 6G are covalently bonded to each other via a triple bond in complex **11**, the emission bands appear at 582 nm and 802 nm with the emission intensity of the 582 nm band dramatically reduced. The red-shifted fluorescence at 802 nm should be attributed to the extended π-conjugation of texaphyrin induced by the triplet bond, which is confirmed by the same emission energy as that of **13**. The reduced intensity of the Rhodamine 6G upconverted fluorescence at 582 nm in **11** upon excitation at 771 nm implies that some degrees of interactions occur between the texaphyrin and Rhodamine 6G components. To verify the interaction between texaphyrin and Rhodamine 6G in complex **11**, the emission of **3**, **11**, **12** and the mixed solution of **3** and **12** at the identical concentration are studied at 550 nm excitation, at which wavelength both the texaphyrin and Rhodamine 6G can be directly excited. As shown in Figure 2b and in Supporting Information Figure S1, upon excitation at 550 nm, **3** exhibits a very strong fluorescence at 582 nm, while **12** and **13** show a very weak fluorescence at 787 nm and 802 nm, respectively. The fluorescence from the mixed solution of **3** and **12** is predominantly from the Rhodamine 6G emission at 582 nm. However, the emission intensity at 582 nm is drastically decreased while the emission at 802 nm is significantly increased in the emission spectrum of **11**

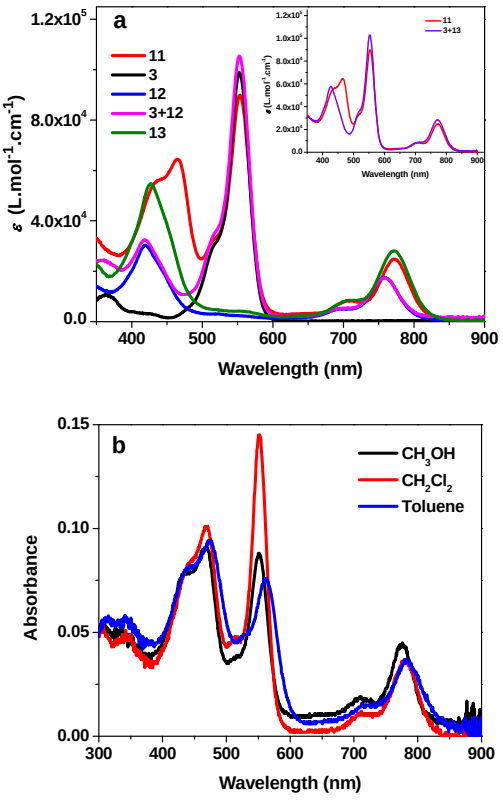

Figure 1. (a) UV-vis absorption spectra of **3**, **11**, **12**, **13**, and the mixture of equivalent **3** and **12,** as well as **3** + **13** at the concentration of 1×10^{-5} mol/L in acetone. (b) UV-vis absorption spectra of **11** in different solvents.

compared to that in respective **3, 12** and **3**+**12** solutions. This indicates that electron transfer or energy transfer from Rhodamine 6G to texaphyrin component occurs. It has been reported that the reduction potential for $[(TXP)Cd]^+$ in acetonitrile is -0.31 V vs Ag/AgCl (corresponding to -0.33 V vs. SSCE) and the oxidation potential is 1.10 V vs. Ag/AgCl (corresponding to 1.08 V vs. SSCE),[34] while the reduction potential for Rhodamine 6G in acetonitrile is -0.50 V vs. SSCE and the oxidation potential is 0.55 V vs. SSCE.[35] According to the equation $\Delta G^0 \approx \text{Ғ} E^0_{D^+/D} - \text{Ғ} E^0_{A/A^-} - E_{*_D} - N_A \frac{e^2}{4\pi\varepsilon_0\varepsilon r}$ (where Ғ is the Faraday constant),[36] the free energy change for electron transfer from the singlet excited state of Rhodamine 6G to texaphyrin is estimated to be approximately -250 kJ/mol; while the back electron transfer from the singlet excited state of texaphyrin to Rhodamine 6G is approximately -220 kJ/mol. Therefore, electron transfer from Rhodamine 6G to texaphyrin is more exothermic and thus feasible in acetonitrile. Although the solvent used in our emission study is acetone, the reduction potentials for Rhodamine 6G and texaphyrin would be different from those in acetonitrile, and thus the ΔG^0 value in acetone would be different from -250 kJ/mol, this estimation still provides valuable information on the feasibility of electron transfer from Rhodamine 6G to texaphyrin in **11**. However, energy transfer from Rhodamine 6G to texaphyrin also likely to occur in view of the overlap of the emission band of Rhodamine 6G and the weak absorption from texaphyrin in the same spectral region. To estimate the fluorescence resonance energy transfer (FRET) efficiency, the quantum yields of the fluorescence band at 582 nm of **3** and **11** in acetone solutions were measured using Rhodamine 6G in ethanol as the reference (Φ_f = 0.95 at λ_{ex} = 480 nm).[37] This gives an Φ_f of 0.29 for **3** and 0.033 for **11** upon excitation at 530 nm (This excitation wavelength was chosen to ensure the primary excitation being the Rhodamine 6G component in **11**), corresponding to an approximately 89% of energy transfer efficiency.

It is worthy of noting that except for excitation at 550 nm, excitation at Soret band (465 nm) and Q-like bands (711 and 771 nm) all gives rise to comparable or stronger fluorescence at 802 nm than that at 582 nm (Figure 2c) for complex **11** due to direct excitation of the texaphyrin component. The fluorescence quantum yields of **11** (including both the emission bands at 582 nm and 802 nm) at different excitation wavelengths were identified to be 0.006 at λ_{ex} = 465 nm, 0.027 at λ_{ex} = 550 nm, 0.003 at λ_{ex} = 711 nm, and 0.0016 at λ_{ex} = 771 nm.

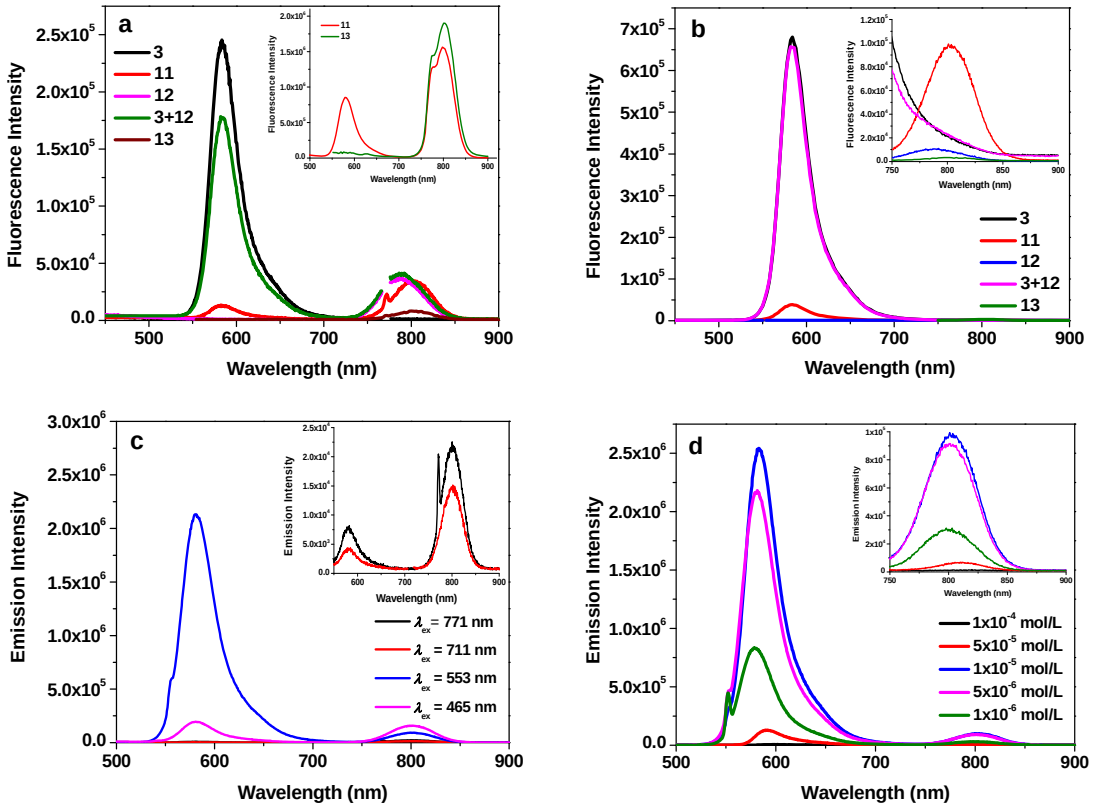

Figure 2. (a) Fluorescence spectra of **3**, **11**, **12**, **13** and the mixture of equivalent **3** and **12** at the concentration of 1×10^{-5} mol/L in acetone, λ_{ex} = 771 nm for all of the samples. Inset shows the comparison of the fluorescence intensity of **11** and **13** under the identical excitation condition of A_{771nm} = 0.05 in a 1-cm cuvette. (b) Fluorescence spectra of **3**, **11**, **12**, **13** and the mixture of equivalent **3** and **12** at the concentration of 1×10^{-5} mol/L in acetone, λ_{ex} = 550 nm for all of the samples. The inset shows the NIR emission band at a larger slit width upon 550 nm excitation. (c) Emission spectra of **11** in acetone at different excitation wavelengths ($c = 1\times10^{-5}$ mol/L). (d) Emission spectra of **11** at different concentrations in acetone, λ_{ex} = 550 nm.

Organic Chemistry Frontiers RSCPublishing

ARTICLE

The concentration-dependent fluorescence study was also carried out for **11** in acetone upon excitation at 550 nm and the results are shown in Figure 2d. The fluorescence intensities of **11** at both 582 nm and 802 nm increase from the concentration of 1×10^{-6} mol/L to 1×10^{-5} mol/L. However, the intensity starts to decrease at the concentration of 5×10^{-5} mol/L. Meanwhile, the emission bands are slightly red-shifted. The decreased fluorescence intensity and slightly red-shifted fluorescence bands are a clear indication of inner-filter effect. However, self-quenching effect cannot be excluded, which could also contribute to the reduced fluorescence intensity at higher concentrations.

Figure 3 shows the fluorescence spectra of complex **11** in different solvents. The energy of the near-IR band is obviously red-shifted in less polar solvents, which is in line with that observed from the UV-vis absorption spectra (Figure 1b). The energy of the emission band at ca. 580 nm does not exhibit a significant change; however, the intensity of this band is dramatically decreased in methanol and toluene.

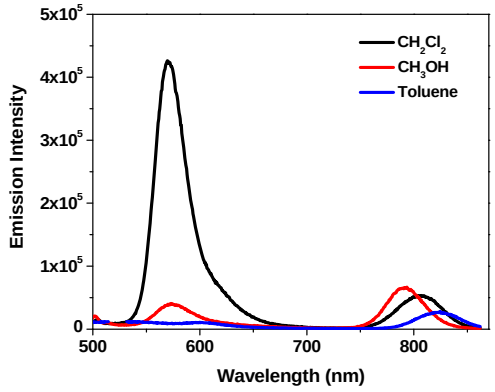

Figure 3. Fluorescence spectra of **11** in different solvents (λ_{ex} = 436 nm). The concentration of the sample solutions were adjusted in order to obtain the same absorbance of 0.08 at 436 nm in a 1-cm cuvette.

Triplet transient absorption (TA). In order to understand the triplet excited-state characteristics, nanosecond transient absorption spectra and the decay characteristics of **3**, **11**, **12**, **13** and the mixture of **3** and **12** were investigated. Figure 4 shows the TA spectra of **3**, **11** – **13** and the mixture of **3** and **12** in acetone at zero delay after 355 nm laser excitation. The TA spectrum from **3** is featured by a very weak positive band between 400 and 500 nm and a strong bleaching band at ~560 nm. The TA spectra of **11** - **13** and **3**+**12** all feature two bleaching bands that correspond to the Soret and Q bands in their respective UV-vis absorption spectra; and a broad, positive absorption band between these two bleaching bands. These features imply that the excited state that gives rise to the observed TA spectra should be the $^3\pi,\pi^*$ state from the texaphyrin. Similar to the trend observed from the UV-vis absorption, the bleaching bands and the positive absorption band of **11** are red-shifted compared to **12**, attributing to the extended π-conjugation by the triple bond. However, the triplet lifetimes obtained from the decay of the TA for all complexes are similar, all on the order of ~12 μs. This indicates that no energy or electron transfer occurs between the texaphyrin and Rhodamine 6G components at the triplet excited state.

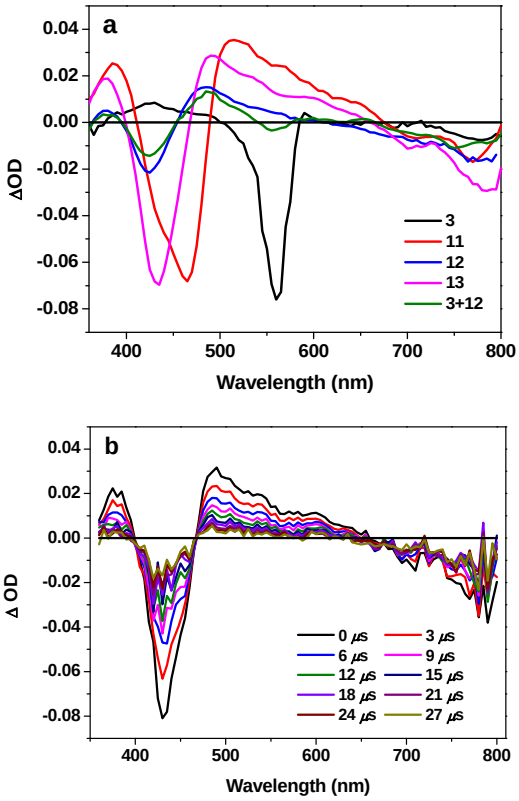

Figure 4. (a) Nanosecond transient difference absorption spectra of **3**, **11-13** and the mixture of **3** and **12** in acetone at zero delay after 355 nm laser excitation. $A_{355\ nm}$ = 0.4 in a 1-cm cuvette for all of the samples. (b) Time-resolved ns TA spectra of **13** in acetone. λ_{ex} = 355 nm, $A_{355\ nm}$ = 0.4 in a 1-cm cuvette.

Conclusions

A texaphyrin derivative with pendant Rhodamine 6G component (complex **11**) via a C≡C bond was synthesized and characterized. The photophysics of this complex and its parent complexes **12** and **13** and Rhodamine 6G derivative **3** were all systematically investigated in acetone solutions at identical experimental conditions. It is found that the UV-vis absorption spectrum of **11** is essentially a simple addition of the absorption spectra of texaphyrin derivative **13** and the Rhodamine 6G derivative **3**, suggesting that no interaction occurs between the texaphyrin component and the Rhodamine 6G component at the ground state. However, when excited at the major absorption band of Rhodamine 6G (550 nm), the

intensity of the 582 nm fluorescence band from the Rhodamine 6G component is dramatically reduced accompanied by a significant increase of the 802 nm band from the texaphyrin component, indicating the occurrence of electron / energy transfer from the singlet excited state of Rhodamine 6G component to the texaphyrin component. The ns TA study suggests that the triplet transient absorption of **11** is dominated by the texaphyrin component, with a long triplet excited-state lifetime ($\tau_T \approx 12$ μs), which implies the lack of interactions between the triplet excited states of Rhodamine 6G component and the texaphyrin component. The broadband ground-state absorption of **11** that covers most of the visible to the near-IR region and the possible electron transfer from the singlet excited state of Rhodamine 6G component to the texaphyrin component suggest that this complex could potentially be used as a broadband photosensitizer for dye-sensitized solar cell applications. Future work will be focused on covering the gap between 600 and 670 nm in the absorption spectrum of **11** and replacing the cadmium central metal ion with the environmentally benign Zn metal ion. For DSSC application, it is also necessary to hydrolyze the ester groups on Rhodamine 6G component to carboxyl groups in order to anchor this sensitizer to the TiO_2 layer.

Experimental section

Synthesis and characterizations. All reagents and solvents were purchased from commercial sources and used as is unless otherwise mentioned. THF and benzene was distilled over sodium. Dichloromethane was distilled over CaH_2.

The synthetic scheme for complex **11** was outlined in Scheme 1. The synthesis of **1**, **2a**, **4a**, **6**, **8**, and **9** followed the literature procedures.[17,25-30] Diamine compounds **2b**, **4b**, and **5b** were synthesized according to the procedures reported by Bahmanyar *et. al*.[38] The synthesis of **2a** and **7** followed the procedures reported by Tour *et. al*.[27] Compound **3** was synthesized via Sonogashira coupling reaction from **1**. Compounds **10** and **11** were obtained following the procedures reported by Sessler *et. al*.[17,31] The synthesis and characterization of complex **12** was reported previously.[32] The synthesis of complex **13** also followed the literature procedure.[17,31] The synthetic details and the characterization data are provided below.

^{1}H NMR was recorded on a 400 or 500 MHz NMR spectrometer at room temperature. ESI-HRMS analysis was conducted on an electrospray ionization / time of flight (TOF) mass spectrometer. Elemental analyses were carried out by a commercial company.

2b. To a rapidly stirred suspension of 1.55 g powdered Zn in 10 mL of concentrated ammonium hydroxide, a 10 mL THF solution containing 4-ethynyl-2-nitroaniline (**2a**) (0.5 mg, 3.07 mmol) was added. The mixture was stirred at room temperature for 2 hours. After the reaction, the reaction mixture was filtered and the mother liquor was washed with diethyl ether. The solvent was then removed, and the residual oil was purified by silica gel column chromatography. The impurity was first removed by CH_2Cl_2 eluent, then elution with ethyl acetate yielded 0.23 g brown oil as the product (yield: 57%). ^{1}H NMR (400 MHz, $CDCl_3$): δ 6.85 (d, J = 7.6 Hz, 1H), 6.76 (s, 1H), 6.50 (d, J = 7.6 Hz, 1H), 3.47 (s, 4H), 2.97 (s, 1H). ^{13}C NMR (100 MHz, $CDCl_3$, TMS) δ 74.5, 84.5, 112.8, 115.9, 120.3, 125.0, 133.9, 136.2. ESI-HRMS Calcd. for $C_{16}H_{17}N_4$ $[2M+H]^+$: 265.1148, Found: 265.1147.

3. Compounds 4-ethynylbenzaldehyde (0.75 g, 5.98 mmol), diester **8** (3.36 g, 11.95 mmol), and *p*-TsOH (0.057 g, 2.98 mmol) were dissolved in 10 mL acetic acid. The reaction mixture was heated to 70 °C and stirred for 12 hours. After the reaction mixture was cooled to r.t., 50 mL water was added. The mixture was extracted by CH_2Cl_2 for three times. The CH_2Cl_2 layers were combined and dried with $MgSO_4$. Then chloranil (0.22 g, 0.90 mmol) was added and stirred at room temperature for 2 hours. After removal of the solvent, the residue was purified by column chromatography (silica gel; CH_3OH/CH_2Cl_2 (1:5 - 1:10 v/v) was used as the eluent) to yield 0.2 g sticky purple solid as the crude product (yield: 5%). Part of the crude product was further purified by preparative TLC plate (silica gel, CH_3OH/CH_2Cl_2 (1:10 v/v)) to afford pure compound **3** as a purple powder (~10 mg), which was used for the photophysical studies. ^{1}H NMR (500 MHz, $CDCl_3$): δ 7.72 (d, J = 7.5 Hz, 2H), 7.39-7.36 (m, 4H), 7.06-7.02 (m, 4H), 3.99 (s, 8H), 3.68 (s, 12H), 3.29 (s, 1H), 2.78 (s, 8H). ^{13}C NMR (100 MHz, $CDCl_3$, TMS) δ 32.1, 47.5, 52.1, 77.2, 98.0, 113.9, 114.9, 117.9, 129.5, 130.3, 131.7, 131.9, 132.6, 155.9, 158.1, 171.5. ESI-HRMS Calcd for $[C_{37}H_{39}N_2O_9]^+$: 655.2650; Found: 655.2632. Anal. Calcd for $C_{37}H_{39}N_2O_9 \bullet CH_2Cl_2 \bullet C_6H_{14} \bullet 1.5H_2O$: C, 61.89; H, 6.85; N, 3.28; found: C, 61.53, H, 6.61; N, 3.95.

4b. Compounds 4-iodo-2-nitroaniline (1.00 g, 3.78 mmol) and NH_4Cl (2.00 g, 37.8 mmol) were dissolved in a mixture of MeOH (20 mL) and THF (20 mL). Zn powder (2.46 g, 37.8 mmol) was then gradually added at 0 °C. The mixture was stirred at room temperature for 40 mins, and then filtered and washed with diethyl ether. After that, the solvent was removed and the residue was recrystallized in $MeOH/CH_2Cl_2$ and hexane to obtain 0.65 g gray solid as the product (yield: 74%). ^{1}H NMR (500 MHz, $CDCl_3$): δ 6.98 (d, J = 8.0 Hz, 1H), 6.94 (s, 1H), 6.41 (d, J = 8.0 Hz, 1H), 3.42 (s, 4H). ^{13}C NMR (100 MHz, $CDCl_3$, TMS) δ 81.3, 118.3, 124.7, 128.7, 134.4, 136.4. Anal. Calcd for $C_6H_7N_2I$: C, 30.79; H, 3.01; N, 11.97; found: C, 31.21, H, 3.43; N, 11.77.

7. Compounds 4-ethynylbenzaldehyde (0.2 g, 1.5 mmol), 5-iodo-2-nitroaniline (0.4 g, 1.5mmol), $Pd(PPh_3)_2Cl_2$ (53 mg, 0.077 mmol), PPh_3 (20 mg, 0.077 mmol) and CuI (14.7 mg, 0.077 mmol) were all added in 10 mL THF and 5 mL triethylamine, and the reaction mixture was degassed. The reaction mixture was stirred at 50℃ for 20 hours. After the reaction, the mixture was washed with brine and dried over $MgSO_4$. Then the solvent was removed, and the residue was purified by column chromatography (silica gel; hexane/CH_2Cl_2 (1:1 v/v) was used as the eluent) to obtain orange powder 0.3 g as the product (yield: 75%). ^{1}H NMR (400 MHz, $CDCl_3$): δ 9.99 (s, 1H), 8.34 (s, 1H), 7.84 (d, J = 8 Hz, 2H), 7.62 (d, J = 8 Hz, 2H), 7.48 (d, J = 8.8 Hz, 1H), 6.79 (d, J = 8.8 Hz, 1H), 6.26 (s, 2H). ^{13}C NMR (100 MHz, $CDCl_3$, TMS) δ 86.2, 87.9, 91.7, 111.2, 119.0, 129.6, 130.0, 131.9, 135.4, 138.2, 144.6, 191.4. Anal. Calcd for $C_{15}H_{10}N_2O_3 \bullet 0.1CH_3COCH_2CH_3 \bullet 0.1C_6H_{14} \bullet 0.8H_2O$: C, 64.67; H, 4.71; N, 9.49; found: C, 64.32, H, 4.82; N, 9.92.

5a. A mixture of compound **7** (2.00 g, 7.50 mmol), diester **8** (4.21 g, 15.02 mmol), and *p*-TsOH (210 mg, 1.12 mmol) in mixed CH_2Cl_2 (20 mL) and acetic acid (50 mL) was heated to 80 °C and stirred for 15 hours. After the reaction mixture was cooled to r.t., 50 mL water was added. Then the mixture was extracted by CH_2Cl_2 for three times. The CH_2Cl_2 layer was combined and dried over $MgSO_4$. After that, chloranil (46 mg, 0.19 mmol) was added to the CH_2Cl_2 solution and the mixture was stirred for 2 hours. After removal of the solvent, the residue was purified by column chromatography for four times (silica gel; CH_3OH/CH_2Cl_2 (1:10 - 1:5 v/v) was used as the eluent.) to yield a purple solid 0.2 g (yield: 3.4%). ^{1}H NMR ($CDCl_3$, 500 MHz) δ 8.01 (s, 1H), 7.66 (s, 2H), 7.65 (d, J = 7.5 Hz, 2H), 7.43 (d, J = 9.5 Hz, 2H), 7.39 (d, J = 7.5 Hz, 2H), 7.13-7.18 (m, 2H), 7.07 (J

= 9.5 Hz, 2H), 7.00 (s, 2H), 4.03 (t, J = 6.0 Hz, 8H), 3.73 (s, 12H), 2.81 (t, J = 6.0 Hz, 8H). ^{13}C NMR (125 MHz, $CDCl_3$, TMS) δ 32.1, 47.6, 52.2, 87.1, 91.6, 97.7, 109.1, 113.7, 114.9, 120.2, 126.1, 129.1, 130.0, 130.1, 130.6, 132.0, 137.2, 146.4, 155.8, 157.9, 171.5. ESI-HRMS Calcd. for $[C_{43}H_{43}N_4O_{11}]^+$: 791.2923, Found: 791.2910.

5b. Compound NH_4Cl (70 mg, 1.30 mmol) and Zn powder (85 mg, 1.30 mmol) were added in a mixture of methanol (10 mL) and THF (10 mL) and stirred vigorously first. Then the solution of **5a** (0.1 g, 0.13 mmol) in 10 mL THF was gradually added at 0 °C. The mixture was stirred at room temperature for 30 mins, and then was filtered and the mother liquor was washed with diethyl ether for three times. After removal of the solvent, the residue was purified by silica gel column chromatography, with mixed CH_3OH/CH_2Cl_2 (1/10 - 1/3 v/v) being used as the eluent. 80 mg purple solid was obtained as the product **5b** (yield: 81%). ^{1}H NMR (400 MHz, $CDCl_3$): δ 7.63 (d, J = 8 Hz, 2H), 7.43 (d, J = 9.2 Hz, 2H), 7.32 (d, J = 8 Hz, 2H), 7.04 (d, J = 9.6 Hz, 2H), 6.97 (s, 2H), 6.82 (d, J = 8.4 Hz, 2H), 6.57 (d, J = 8Hz, 1H), 3.97 (s, 8H), 3.67 (s, 12H), 2.75 (t, J = 6.4 Hz, 8H). ^{13}C NMR (125 MHz, $CDCl_3$, TMS) δ 32.1, 47.6, 52.2, 91.4, 93.0, 97.9, 109.7, 111.4, 113.7, 114.8, 119.9, 126.0, 129.4, 129.9, 130.66, 130.7, 131.8, 132.0, 137.8, 145.9, 155.9, 158.0, 171.5. ESI-HRMS Calcd. for $[C_{43}H_{45}N_4O_9]^+$: 761.3181, Found: 761.3195.

10. Compounds **9** (95 mg, 0.21 mmol) and **5b** (163 mg, 0.21 mmol) were dissolved in a degassed mixture of 100 mL dry toluene and 25 mL absolute methanol. Concentrated HCl (0.05 mL) was then added and the resulting dark brown solution was heated to reflux for 24 hours under argon atmosphere. A water segregator was used to remove the water generated from the reaction. After cooling, K_2CO_3 (50 mg) was added to neutralize the HCl and the solution was then filtered through $MgSO_4$. The solvent was then removed and the residue was dissolved in 10 mL CH_2C1_2. Addition of 30 mL hexane precipitated out some sticky dark brown solid. This solid was recrystallized with CH_2Cl_2/hexane multiple times, which yielded dark red powder 103 mg (yield: 43%). This compound was directly used for the next step reaction without further purification. ESI-HRMS Calcd for $[C_{68}H_{74}N_7O_9]^+$: 1132.5543, Found: 1132.5508.

11. Compound **10** (100 mg, 0.088 mmol) was dissolved in 20 ml $CHCl_3$, and $Cd(NO_3)_2$•$4H_2O$ (81.7 mg, 0.26 mmol) was dissolved in 50 ml methanol. The two solutions were mixed together and were heated to reflux for 72 hours while bubbling with air. UV-vis spectroscopy was used to monitor the reaction. During the reaction, the 375 nm peak corresponding to the ligand **10** gradually disappeared, while the Q band at ~770 nm originating from **11** kept increasing. The reaction was stopped when no more change of the Q band intensity was observed. After the reaction, the solvent was removed and the residue was dissolved in CH_2Cl_2 and washed with water, and then dried over $MgSO_4$. CH_2Cl_2 was removed and the residue was purified by silica gel column chromatography with CH_3OH/CH_2Cl_2 (1/30 - 1/5 v/v) being used as the eluent, which yielded 30 mg purple solid. Further purification of these solids using preparative TLC plate (silica gel, CH_3OH/CH_2Cl_2 (1/5 v/v) was used as the eluent), and recrystallization from methanol and ethyl acetate afforded 10 mg reddish brown powder as the pure product (yield: 8.7%). ^{1}H NMR (400 MHz, $CDCl_3$): δ 10.58 (s, 1H), 10.50 (s, 1H), 9.02 (s, 3H), 8.72 (s, 1H), 7.89 (s, 2H), 7.77 (s, 1H), 7.51 (s, 4H), 7.14 (s, 2H), 6.99 (s, 2H), 3.94 (s, 8H), 3.68 (s, 12H), 3.35 (s, 6H), 2.92 (s, 3H), 2.77 (s, 8H), 2.61 (s, 3H), 2.42 (s, 3H), 1.53 (m, 9H). ^{13}C NMR (125 MHz, $CDCl_3$, TMS) δ 17.3, 19.1, 29.3, 2.7, 32.2, 47.7, 52.1, 87.9, 90.8, 97.4, 109.2, 113.61, 113.64, 113.9, 115.35, 115.42, 116.77, 116.81, 125.66, 125.69, 127.8, 130.5, 132.5, 136.9, 138.7, 139.5, 145.6, 146.56, 146.62, 149.3, 150.9, 154.6, 155.7, 157.7, 171.7. ESI-HRMS Calcd for $[C_{68}H_{69}CdN_7O_9]^+$: 620.7100; Found: 620.7089. Anal. Cacld for $C_{68}H_{69}CdN_8O_{12}\cdot 2CH_2Cl_2\cdot 6CH_3OH$: C, 55.52; H, 6.19; N, 6.56; found: C, 55.63; H, 6.21; N, 6.24.

13. Compounds **9** (200 mg, 0.49 mmol) and **2b** (64 mg, 0.49 mmol) were dissolved in a degassed mixture of 100 mL dry toluene and 25 mL absolute methanol. 0.05 mL concentrated HCl was then added and the resulting yellowish brown solution was heated to reflux for 24 h under nitrogen atmosphere. A water segregator was used to remove the water generated from the reaction. After cooling, K_2CO_3 (20 mg) was added to neutralize the HCl and the solution was then filtered through $MgSO_4$. After removal of the solvent, the residue was recrystallized from CH_2Cl_2/hexane to give 200 mg dark brown powder, which was confirmed by the MS (m/z = 503.29) to be the desired macrocyclic ligand (yield: 81%). This ligand was directly used for the next step reaction without further purification.

The obtained ligand (200 mg, 0.40 mmol) was dissolved in 20 ml $CHCl_3$, and $Cd(NO_3)_2$•$4H_2O$ (320 mg, 1.04 mmol) was dissolved in 50 ml methanol. These two solutions were mixed together and the reaction mixture was heated to reflux for 72 hours while bubbling with air. During the reaction, the 365 nm peak corresponding to the ligand gradually disappeared, while the Q band at ~770 nm emanating from **13** kept increasing. The reaction was stopped when the intensity of the Q band no longer changed. After the reaction, the solvent was removed and the residue was purified by silica gel column chromatography with CH_2Cl_2/acetone (1:20 v/v) being used as the eluent. Further purification via recrystallization from CH_2Cl_2/hexane yielded 100 mg dark yellow solid (yield: 37%). ^{1}H NMR (500 MHz, $CDCl_3$): δ 11.28 (s, 2H), 9.58 (m, 1H), 9.41 (m, 1H), 9.28 (d, 1H), 8.38 (m, 2H), 3.55-3.50 (m, 12H), 3.08-3.07 (m, 4H), 1.66-1.52 (m, 9H). ESI-HRMS Calcd for $[C_{33}H_{32}CdN_5+H_2O]^+$: 630.1800; Found: 630.1766.

Photophysical Measurements. UV-vis spectra were measured on a UV-VIS recording spectrophotometer in a 1-cm quartz cuvette. Steady-state fluorescence spectra at room temperature were measured on a fluorometer. The excitation wavelength was selected at the respective absorption band maxima. Spectrophotometric grade acetone was used as the solvent. A comparative method[39] was used to determine the fluorescence quantum yield, with Rhodamine 6G in ethanol (Φ_f = 0.95 at λ_{ex} = 480 nm)[37] being used as the reference. The nanosecond transient difference absorption (TA) spectra and triplet excited-state lifetimes were measured in degassed acetone solutions on a laser flash photolysis spectrometer. The third harmonic output (355 nm) of a Nd:YAG laser (4.1 ns, repetition rate was set at 1 Hz) was used as the excitation source. Each sample was purged with argon for 30 min prior to measurement.

Notes and references

[a] Department of Chemistry and Biochemistry, North Dakota State University, Fargo, ND 58108-6050, USA. E-mail: Wenfang.Sun@ndsu.edu

[b] College of Chemistry and Chemical Engineering, Hubei University, Wuhan 430062, P. R. China

Electronic Supplementary Information (ESI) available: Fluorescence spectra of **3**, **11**, and **13** in acetone under the identical excitation condition of A_{550nm} = 0.05 in a 1-cm cuvette. ^{1}H and ^{13}C NMR spectra of reported

compounds **2b**, **3**, **4b**, **7**, **5a**, **5b**, and **11**, and ^{1}H NMR spectrum of **13**. See DOI: 10.1039/b000000x/

1 B. O'Regan and M. Grätzel, *Nature*. 1991**, 353**, 737.
2 C.-Y. Chen, M. Wang, J.-Y. Li, N. Pootrakulchote, L. Alibabaei, C.-h. Ngoc-le, J.-D. Decoppet, J.-H. Tsai, C. Grätzel, C.-G. Wu, S. M. Zakeeruddin and M. Grätzel, *ACS Nano* 2009, **3**, 3103.
3 F. Odobel and H. Zabri, *Inorg. Chem.* 2005, **44**, 5600.
4 K. Kalyanasundaram, *Photochemistry of Polypyridine and Porphyrin Complexes*, Academic Press: London, 1992.
5 X.-F. Wang, L. Wang, N. Tamai, O. Kitao, H. Tamiaki and S.-I. Sasaki, *J. Phys. Chem. C* 2011, **115**, 24394.
6 X.-F. Wang and H. Tamiaki, *Energy Environ. Sci.* 2010, **3**, 94.
7 H. Imahori, T. Umeyama and S. Ito, *Acc. Chem. Res*. 2009, **42**, 1809.
8 X.-F. Wang, H. Tamiaki, L. Wang, N. Tamai, O. Kitao, H. Zhou and S.-I. Sasaki, *Langmuir* 2010, **26**, 6320.
9 X.-F. Wang, O. Kitao, H. Zhou, H. Tamiaki and S.-I. Sasaki, *J. Phys. Chem. C* 2009, **113**, 7954.
10 M. G. Walter, A. B. Rudine and C. C. Wamser, *J. Porphyrins Phthalocyanines* 2010, **14**, 760.
11 V. S. Lin, S. G. DiMagno and M. J. Therien, *Science* 1994, **264**, 1105.
12 M. Nappa and J. S. Valentine, *J. Am. Chem. Soc*. 1978, **100**, 5075.
13 P. Bhyrappa and V. Krishnan, *Inorg. Chem*. 1991, **30**, 239.
14 Y. Tachibana, S. A. Haque, I. P. Mereer, J. R. Durrant and D. R. Klug, *J. Phys. Chem. B* 2000, **104**, 1198.
15 T. Bessho, S. M. Zakeeruddin, C.-Y. Yeh, E. W.-G. Diau and M. Grätzel, *Angew. Chem.* 2010, **122**, 6796; *Angew. Chem. Int. Ed.* 2010, **49**, 6646.
16 A. Yella, H.-W. Lee, H. N. Tsao, C. Yi, A. K. Chandiran, Md. K. Nazeeruddin, E. W.-G. Diau, C.-Y. Yeh, S. M. Zakeeruddin and M. Grätzel, *Science* 2011, **334**, 629.
17 J. L. Sessler, M. R. Johnson and V. Lynch, *J. Org. Chem*. 1987, **52**, 4394.
18 J. L. Sessler, T. D. Mody, G. Hemmi and V. Lynch, *Inorg. Chem*. 1993, **32**, 3175.
19 J. L. Sessler, G. Hemmi, T. D. Mody, T. Murai, A. Burrell and S. W. Young, *Acc. Chem. Res*. 1994, **27**, 43.
20 T. Lu, P. Shao, I. Mathew, A. Sand and W. Sun, *J. Am. Chem. Soc.* 2008, **130**, 15782.
21 B. G. Maiya, T. E. Mallouk, G. Hemmi and J. L. Sessler, *Inorg. Chem*. 1990, **29**, 3738.
22 Y. Ooyama and Y. Harima, *Eur. J. Org. Chem*. 2009, 2903.
23 W. Lin, L. Yuan, Z. Cao, Y. Feng and J. Song, *Angew. Chem.* 2010, **122**, 385; *Angew. Chem. Int. Ed*. 2010, **49**, 375.
24 K. Krishnamoorthy and T. P. Begley, *J. Am. Chem. Soc*. 2010, **132**, 11608.
25 L. Huang, L. Zeng, H. Guo, W. Wu, W. Wu, S. Ji and J. Zhao, *Eur. J. Inorg. Chem*. 2011, 4527.
26 D. W. Jr. Price, S. M. Dirk, F. Maya and J. M. Tour, *Tetrahedron* 2003, **59**, 2497.
27 F. Maya, S. H. Chanteau, L. Cheng, M. P. Stewart and J. M. Tour, *Chem. Mater*. 2005, **17**, 1331.
28 F. Maya and J. M. Tour, *Tetrahedron* 2004, **60**, 81.
29 Y. Chen, Y. Wu, P. Henklein, K. Nakanishi, X. Li, O. P. Ernst and K. P. Hofmann, *Chem. Eur. J.* 2010, **16**, 7389.
30 R. Bandichhor, A. D. Petrescu, A. Vespa, A. B. Kier, F. Schroeder and K. Burgess, *Bioconjugate Chem*. 2006, **17**, 1219.
31 J. L. Sessler, T. Murai, V. Lynch and M. Cyr, *J. Am. Chem. Soc.* 1988, **110**, 5586.
32 W. F. Sun and D. Y. Wang, *Chin. Chem. Lett*. 1993, **4**, 225.
33 P. J. Schuck, K. A. Willets, D. P. Fromm, R. J. Twieg and W. E. Moerner, *Chem. Phys.* 2005, **318**, 7.
34 B. G. Maiya, A. Harriman, J. L. Sessler, G. Hemmi, T. Murai and T. E. Mallouk, *J. Phys. Chem*. 1989, **93**, 8111.
35 L. Bahadur and P. Srivastava, *Solar Energy Mater. Solar Cells* 2003, **79**, 235.
36 N. J. Turro, V. Ramamurthy and J. C. Scaiano, *Modern Molecular Photochemistry of Organic Molecules*, University Science Books, Sausalito, CA, Chapter 7, p. 421, 2010.
37 R. F. Kubin and A. N. Fletcher, *J. Luminescence* 1982, **27**, 455.
38 S. Bahmanyar, R. J. Bates, K. Blease, A. A. Calabrese, T. O. Daniel, M. Delgado, J. Elsner, P. Erdman, B. Fahr, G. Fercuson, B. Lee, L. Nadolny, G. Packard, P. Papa, K. V. Plantevin, J. Riggs, P. Rohanf, S. Sankar, J. Sapienza, Y. Satoh, R. Stevens, L. Tehrani, J. Tikhe, E. Torres, A. Wallace, B. W. Whitefield and J. Zhao, *PCT Int. Appl.* 2010, 2010027500.
39 J. N. Demas and G. A. Crosby, *J. Phys. Chem.* 1971, **75**, 991.